Cavity Gas Analysis for Light Ion Beam Fusion Reactors

R.R. Peterson, G.W. Cooper, and G.A. Moses

August 1980

UWFDM-371

Nucl. Technology/Fusion 1, 377 (1981).

FUSION TECHNOLOGY INSTITUTE

UNIVERSITY OF WISCONSIN

MADISON WISCONSIN

Cavity Gas Analysis for Light Ion Beam Fusion Reactors

R.R. Peterson, G.W. Cooper, and G.A. Moses

Fusion Technology Institute
University of Wisconsin
1500 Engineering Drive
Madison, WI 53706

http://fti.neep.wisc.edu

August 1980

UWFDM-371

Nucl. Technology/Fusion 1, 377 (1981).

CAVITY GAS ANALYSIS FOR

LIGHT ION BEAM FUSION REACTORS

R. R. PETERSON
(University of Wisconsin)

G. W. Cooper
(University of New Mexico)

G. A. Moses
(University of Wisconsin)

Fusion Engineering Program
Nuclear Engineering Department
University of Wisconsin
Madison, WI 53706

August 1980

UWFDM-371

I. INTRODUCTION

Inertial confinement fusion has been studied in the U.S. since the mid-1960's with disclosure of the fundamental concept, compressing the DT fuel to super-high densities, coming in the landmark paper of Nuckolls, et al., in 1972.[1] To achieve this high compression, complex targets consisting of DT fuel encapsulated within surrounding spherical shells of other materials such as glass or gold must be irradiated by an energy source of very high intensity ($\sim 10^{14}$ - 10^{16} W/cm^2). High power lasers have achieved notable success in driving these targets to high compressions and have received the greatest amount of attention thus far in the quest for breakeven conditions.[2]

Another source of energy at high intensities that has been applied to inertial fusion target experiments is pulsed relativistic electron beams.[3] In these experiments the target is actually mounted on the anode of a large pulsed power device and the electrons are focused onto it. However, this approach to ICF suffers from some serious problems related to focusability of the electrons onto a small target and the range of electrons in matter. Historically, pulsed power generators of relativistic electrons have been used to produce hard X-ray bursts to simulate nuclear weapons effects. For this purpose the electron intensity has proven to be adequate. However, the further increase in intensity required for ICF applications has raised doubts about the pulsed power-REB approach.

Most, if not all, of these problems have been potentially solved by the demonstration that the same pulsed power technology can be used to accelerate light ions rather than electrons.[4] Light ions such as H^{+1} or He^{+2} at comparable energies of 1-10 MeV have much shorter ranges in matter and can in principle be bunched to provide a higher intensity than electrons. With these

more optimistic driver characteristics it is becoming increasingly apparent from target design calculations that light ions are a very effective source of pulsed energy for ICF applications.[5]

The light ion beam (LIB) approach to ICF does have one common problem with its forerunner, the REB approach. This involves the target irradiation geometry. In each case, the target is either an internal part of the diode or is close enough (50 cm) that the ions can be ballistically focused onto it. This should be adequate for experiments up to and including the breakeven stage, but it certainly does not extrapolate to the reactor stage where yields of 100 MJ at repetition rates of 10 Hz are required or to nearer term high gain target development facilities. In these cases the rather massive diode structure would likely be quickly destroyed by the blast from the exploding target.

Clearly the "standoff" distance between the target and the final diode or diodes must be several meters for such future applications. This problem has a potential solution in the form of plasma channels that allow the ion beams to "conduct" in a charge and current neutralized state from the diodes to the target.[4,6] In experiments, these discharge plasma channels have been created by exploding thin wires in a background gas introduced into the target chamber.[7] For reactor applications, where a repetition rate capability is necessary, it has been proposed to pre-ionize the channels with laser beams and then discharge capacitors through the channels to provide the current needed for confinement of the ions.[6] This is schematically shown in Fig. 1.

A very critical component of this ion beam propagation scheme is the background gas in which the channels are formed. It must have all of the characteristics needed for effective pre-ionization by the laser beams and for

efficient ion beam propagation once the channel is fully formed. Furthermore, for hydrodynamic as well as charge and current neutralization purposes the gas will be in a pressure range of 10-100 Torr where it will very effectively attenuate the target debris ions and X-rays once the target explodes. This will of course protect the first wall of the reactor from direct irradiation by the target debris and X-rays. This is a very positive result since first wall protection is a serious problem in all ICF reactor designs.[8] However, the rapid deposition of energy into the background cavity gas will generate a fireball with its resulting radiative heat flux and blast wave overpressure. The first wall must then be designed to accommodate this fireball. The details of the fireball behavior, and hence the first wall design, will depend upon the equation of state and radiative properties of the gas. Therefore, the choice of cavity gas must also address the response to the target explosion.

The choice and analysis of cavity gases that meet the combined criteria of channel formation, ion propagation and fireball response are the subject of this paper. In Section II, we review possible laser ionization mechanisms and relate these to specific choices for the cavity gas. In Section III, these gas choices are analyzed from the perspective of fireball dynamics and first wall response. Section IV includes a list of specific gas parameters that appear to meet all of the identified criteria for reactor applications. This last part also pertains to the conclusions of the study and suggestions of further work in this area.

II. LASER GUIDED PLASMA CHANNELS

An essential feature of a light ion beam fusion reactor is the efficient transport of the beam from the accelerator diode to the fusion target. This

transport distance must be several meters in order to protect the diode from the microexplosion. Ion beams can be efficiently transported over this distance if they propagate inside a preformed plasma channel that provides both beam current neutralization and a sufficient azimuthal magnetic field to guide the beam.[7,9-10] These plasma channels must also be relatively straight and free of inhomogeneities if the ion beam is to remain stable. Since discharges tend to naturally form curved, kinked paths, the discharge must be externally guided to form the straight, smooth channels required. Experimentally, ions have been propagated along channels guided by wires[7] and wall-confined discharges[9] but neither of these approaches is suitable for a repetitively pulsed reactor. It has been proposed that a laser guided discharge would be a more viable approach.[6,7] To evaluate this suggestion, the various processes by which a laser might guide a discharge are examined and one of the more attractive processes is investigated in detail.

A laser may guide a discharge by ionizing the gas (by any of several different processes), by creating a rarefaction channel, or by producing a large excited state population. Each of these must be evaluated in light of the external constraints that will be imposed by other aspects of the reactor design. The laser process must guide the discharge over the entire path ($\geq$ 4 m), produce a small initial channel diameter ($\sim$ 2 mm), and result in a channel that is relatively straight and free of inhomogeneities. The ability of a process to meet these requirements will depend significantly on the reactor gas composition because processes are dependent on species, density, which affects laser energy and power requirements, turbulence[11], and temperature, which affects background ionization density and molecular and gas kinetic processes.

There are many laser processes that could ionize a gas including multiphoton ionization, cascade ionization, aerosol initiated ionization, direct photo-ionization, two photon ionization, and resonance absorption/ electron run-away processes. Each of these have been examined and are discussed below. Following the ionization processes the rarefaction channel and excited state population processes will be discussed.

MULTIPHOTON IONIZATION: In this process an atom or molecule is ionized by absorbing, almost simultaneously, a number of photons whose individual energies are insufficient to ionize the gas. Because the process relies on a succession of excitations through a series of (usually) very short-lived virtual states, the process requires very large photon fluxes to become significant. In fact, there exists an intensity threshold ($\gtrsim 10^{10}$ W/cm^2) below which multiphoton ionization is insignificant.[12] This intensity threshold will make it difficult to obtain ionization along the entire channel length, although methods of rapidly sweeping the laser focus may make this possible.[13] Because the process is inefficient, 100's and possibly even 1000's of joules of incident laser energy will be required per channel.[14,15] Also a significant fraction of this energy will pass through the gas and strike the fusion target. This will require specially designed targets that can tolerate such energies, adding complexity to an already difficult problem. Finally, it has been observed[14-16] that radial shock waves form, causing the plasma to expand at velocities of 0.1 to 1. cm/μsec. This could result in final plasma channel diameters that are too large for efficient ion beam propagation. Thus, multiphoton ionization does not appear to be a promising mechanism for initiating plasma channels unless a suitable method of sweeping the focus is found.

CASCADE IONIZATION: In this process a free electron is accelerated by the laser electromagnetic field until it has enough energy to ionize an atom or molecule. These two electrons in turn are accelerated until they ionize two more atoms or molecules. For this cascade to occur, the gas density must be high enough ($\geq 10^{18}$ cm^{-3}) that the electron collisional mean free path is much shorter than the dimensions of the region of high laser electromagnetic field.[12] Like multiphoton ionization, it has an intensity threshold,[12] although it is somewhat lower ($\geq 10^{8}$ W/cm^2). It also suffers many of the same problems as multiphoton ionization; it will be difficult to ionize the entire channel length, it will require large laser energies, it will significantly irradiate the target, and it will generate a radial shock wave upon gas breakdown. Also the anticipated gas densities ($\sim 10^{18}$ cm^{-3}) in a light ion beam reactor will be barely sufficient for the process to occur. Thus, cascade ionization also does not appear promising.

AEROSOL INITIATED IONIZATION: It has been found that a laser beam interacting with aerosols results in plasma formation. This process also has an intensity threshold ($\sim 10^{6}$ W/cm^2) but it is much lower than either cascade or multiphoton ionization. This mechanism has been used to guide discharges over significant distances.[17-20] The initial experiments required substantial laser energies[17-18] (350 to 400 J/m) but in recent work the energy requirement has been greatly reduced[19,20] ($\sim$ 15 J/m). Some potential problems include laser energy reaching the target, the time required to obtain a uniform channel density (it may take longer than turbulence effects will allow), the survivability of aerosols if the cavity gas temperature is high, and the effect of aerosols on the ion beam propagation if the aerosols survive the discharge. Advantages include the fact that a practical laser

such as CO_2 could be used and that the energy requirements are reasonable, particularly for an efficient laser such as CO_2. Overall, aerosol initiated ionization appears to be a reasonably attractive process.

DIRECT PHOTO-IONIZATION: In direct photo-ionization a single photon has sufficient energy to ionize the atom or molecule directly. This process does not have a threshold so that much lower laser energy and power requirements would be expected for direct photo-ionization than for the above processes. However, the laser photon energy requirement will place strict limitations on laser wavelength and cavity gas. For the atom with the lowest ionization potential (Cs, ~ 3.8 eV), the maximum allowable wavelength is about 300 nm. For gases having higher ionization potentials, the wavelength would have to be even shorter. The problem of requiring a gas with a low ionization potential may be partially ameliorated by using a two-component gas. This will allow the more practical situation of a low ionization potential alkali vapor in a higher pressure gas. Providing a practical UV laser system is available, this is also a reasonably promising approach.

TWO PHOTON IONIZATION: In this process an atom or molecule is ionized by absorbing two photons, not necessarily of the same energy. This differs from a two-step multiphoton process in that the laser wavelength is tuned to a specific transition of the atom or molecule. The cross section for this absorption can be large and the lifetime of the state relatively long so that the gas can be ionized with relatively low laser energy and power requirements. This would have the advantage over direct photo-ionization in that the laser wavelength, gas specie requirement or both could be relaxed. However, if two different wavelengths (lasers) are required there will be the problem of obtaining collinearity of the beams and the added complexity of having two laser systems.

RESONANCE ABSORPTION/ELECTRON RUN-AWAY: In these processes the laser is again tuned to a specific transition of the gas atom or molecule. By saturating this transition, a large excited state population is created, either by direct absorption by an atom or by dissociating molecules that selectively yield excited atoms. If free electrons are present, they will be heated via super-elastic collisions with the excited atoms. After a few such collisions the electrons will have enough energy to ionize the atoms. These processes have large cross sections and can be very rapid so again the laser energy and power requirements should be low. Although almost any atomic gas could be used, to minimize energy requirements, gases with low ionization potentials are preferable (i.e., alkali vapors). A thorough search for suitable molecules has not been undertaken but molecules such as OCSe and OCS that were investigated for Group VI lasers are potential candidates. A question to be answered for any molecular process is whether the molecules survive the microexplosion, either directly or by recombination. If they do not survive, the question becomes whether they can be replaced between shots. A positive answer is needed to at least one of these questions if a molecular process is to be a viable candidate for guiding the discharges. A minor problem with this approach is that tunable lasers would have to be used.

RAREFACTION CHANNEL: In this approach a molecular gas is used that strongly absorbs the laser radiation. This rapidly heats the gas, causing it to expand, leaving an under-dense channel. The combination of lower density and higher temperature is sufficient to guide a discharge.[21] This process requires a minimal amount of laser energy and power and could use a practical laser such as CO_2. However, there is some question as to whether this process will provide sufficient inducement to guide a discharge in a reactor environ-

ment with its close ground planes and high temperature, partially ionized chamber gas. Also, the time required to establish the channel may prove too long with respect to turbulence effects. Although there are potentially serious problems with this approach, the advantages are such that it warrants further investigation.

LARGE EXCITED STATE POPULATION: It has been suggested, but not proven, that producing a large excited state population along the desired path will guide a discharge because the ionization potential of these atoms or molecules has been effectively lowered. One possible approach uses ammonia, which has the property that energy absorbed as vibrational energy will rapidly partition into electronic states.[22] As with rarefaction, there is some doubt as to whether this process could guide a discharge in the reactor environment. Also, if ammonia were used, its large hydrogen content could greatly complicate tritium recovery. Thus, like the case of the rarefaction channel, there are potentially serious problems with this approach but it also warrants further examination.

Any of the above processes, under the proper conditions, could probably be used to guide a discharge. However, multiphoton and cascade ionization seem least favorable, primarily due to their apparent large laser energy and power requirements. The rarefaction channel and excited state population approaches are attractive but seem to present the most serious questions regarding their ability to guide a discharge in a reactor environment. The remaining processes are all promising and appear roughly comparable, each having specific advantages and disadvantages. Since the ultimate constraints that will be imposed are not well defined, it would not be meaningful to try to select the optimal process from among these without doing an evaluation of

each in conjunction with other reactor design elements. It should also be noted that an optimal process for a reactor would be expected to be different than one for a single shot, experimental machine. To begin an integrated evaluation, resonance absorption/electron run-away was selected. From the initial evaluation, these processes seem to meet the necessary requirements, to be applicable over a relatively wide range of possible reactor conditions, and to present fewer unknowns than some of the other processes. The particular process selected was resonance absorption in atomic sodium.

Experimentally, sodium,[23] lithium,[24] and cesium[25] have all been fully ionized by irradiating the alkali vapors (densities of about 10^{16} cm^{-3}) with lasers of modest energies tuned to resonance transitions of the respective species. These experiments demonstrate both the effectivenss of this process to ionize the vapors and indicate that the various alkali vapors should behave similarly. Thus, the results presented for sodium should be representative of the behavior of other alkali vapors.

The basic process can be described as follows. A dye laser is tuned to the $3^2S_{1/2}$ to $3^2P_{1/2}$ transition (λ = 589.6 nm) of the sodium atom. The laser power and energy are adjusted such that the transition is saturated, creating a large excited state population. Free electrons, possibly generated by multiphoton ionization of the excited atoms, are heated via super-elastic collisions with the excited atoms. After undergoing two or three such collisions the electrons will have enough energy to ionize the excited or ground state atoms respectively. Other processes will undoubtedly contribute to the total ionization, but these should be the dominant ones.[26,27] Both the photon absorption and electron collisional processes have large cross sections so that full ionization can be achieved very rapidly.[23,26-27] Experimen-

tally a 10 cm column of sodium at ~ 10^{16} cm^{-3} was fully ionized by a 1 MW, 500 nsec laser pulse.[23]

This process has been modeled by Measures, et al.[26-27] and their results are in qualitative agreement with experiment.[23] Their results[26] for the time required to reach 75% ionization versus laser irradiance and sodium density and for the maximum laser power absorbed per unit volume versus sodium density were used in this study. Since they presented results for only three sodium densities (10^{15}, 10^{16}, and 10^{17} cm^{-3}), values for parameters corresponding to other densities are obtained by interpolation. It was felt that interpolation would provide sufficient accuracy for this study since the model results had not been normalized to experimental results.

To evaluate this process for reactor conditions it is necessary to obtain an estimate of the laser energy and pulse width requirements for a typical channel as a function of sodium density. This can be done by following the approach used by Measures, et al.[26] Knowing the time required to reach 75% ionization (this is essentially the same time that is required to reach full ionization as the process becomes very rapid after the electron density reaches a threshold value)[26] as a function of laser irradiance and sodium density and the maximum power absorbed per unit volume (Q_{max}), one can calculate the irradiance I(Z) at a distance Z into the plasma as

$$I(Z) = I_o - Q_{max}Z \qquad (1)$$

where the initial irradiance is I_o. Assuming that the laser pulse width, τ, is equal to the ionization time, then the laser energy density, E, can be found:

$$E \geq \tau I_o \tag{2}$$

For sodium densities of interest (10^{14} to 10^{16} cm^{-3}) the laser pulse width can be given approximately by

$$\tau \geq \frac{\beta}{[I]^m} \tag{3}$$

where β and m are constants that are functions of sodium density (see reference 26). Since the ionization time increases as the irradiance decreases, the laser pulse must be at least as long as the ionization time corresponding to the lowest irradiance or $I(\ell)$ where ℓ is the length of the channel. Therefore we get

$$\tau \geq \frac{\beta}{[I(\ell)]^m} = \frac{\beta}{[I_o - Q_{max}\ell]^m} \tag{4}$$

and

$$E \geq \tau I_o = \frac{I_o \beta}{[I_o - Q_{max}\ell]^m} \tag{5}$$

Equation 4 estimates the laser pulse width required for a channel of length ℓ and Eq. 5 estimates the laser energy density. Multiplying the energy density by the channel area will give the total laser energy required.

Laser energy density versus laser pulse width for several sodium densities is plotted in Fig. 2 for a typical channel length of 5 meters. The

vertical scale to the right gives the total energy required for a uniform channel area of 0.2 cm^2. This area represents the largest initial channel area that one would wish to consider and thus represents a "maximum" energy requirement. Note that for each sodium density, the energy required goes through a minimum giving the ideal operating point. For a 0.2 cm^2 area, the minimum laser energy requirements range from ~ 2 J at 10^{16} cm^{-3} down to ~ 0.4 J at 5×10^{14} cm^{-3}. Since the minimum energy decreases as the sodium density decreases, one would wish to operate at as low a density as possible from the point of view of the laser system. However, since the laser pulse width increases for decreasing sodium densities, there will be a minimum density cut-off (~ 5×10^{14} cm^{-3}) due to turbulence effects. The discharge must be initiated before turbulence has time to distort the channel. This time may be as short as one microsecond.[11] A more severe density limit, however, results from the need to protect the first wall from the micro-explosion. As the fireball calculations of Section III will indicate, the sodium density should be at least ~ 10^{15} cm^{-3}. Another restriction is that ion beam transport requires densities of about 10^{18} cm^{-3} but laser pulse width limitations and practical problems of attaining higher densities will limit sodium densities to < 10^{16} cm^{-3}. Thus, a buffer gas such as argon must be added to the sodium to attain the required density. A preliminary examination indicates that the argon should not adversely affect the laser guiding process but this should be examined more closely.

It is also necessary to calculate the total laser system energy requirements. We assume that the laser system should require not more than about 2% of the total stored ion accelerator energy. For our reference accelerator design the stored energy is 8 MJ so that the maximum allowable laser system

energy is 160 kJ. It will also be assumed that there are 40 discharge channels, each having a length of 5 m and an area of 0.2 cm^2. Two sodium densities, 1 and 5 x 10^{15} cm^{-3}, will be used to indicate the range of laser energies required.

From Fig. 2 it can be seen that the minimum laser energies required to initiate these channels at 1 x 10^{15} and 5 x 10^{15} cm^{-3} sodium densities are 1 and 1.5 J, respectively. Since the energy curves are fairly flat at the minimums the laser pulse widths could vary from about 200 to 600 nsec at a density of 10^{15} cm^{-3} and 50 to 100 nsec at 5 x 10^{15} cm^{-3}. For forty channels the total laser energies incident on the gas will be 40 and 60 J. A conservative estimate for the dye laser efficiency is ~ 0.1%, giving total system energies of 40 and 60 kJ for the two cases. Both are well below the design limit of 160 kJ. In addition, a more desirable channel area of 0.1 cm^2 would reduce the energy requirements by a factor of two. Also a somewhat more efficient dye laser could be expected.[28]

An important question to consider is whether dye lasers can meet the above requirements. With respect to total energy delivered per channel and pulse width, there are off-the-shelf dye lasers that essentially meet these requirements.[29] There appears to be no fundamental reason why they cannot meet beam quality and pulse repetition rate requirements as well. It can also be noted that a very common dye, Rhodamine-6G, is ideal for producing the 589.6 nm wavelength required for sodium. The extensive developments in the area of high-energy, high-average-power, dye lasers for chemical processing[28] should also be relevant to this application.

Although this approach appears quite promising, there are several questions that remain to be answered. One is how effectively the process

could guide a discharge in a reactor environment. Sodium vapor itself is a relatively highly conducting gas and there will be many unavoidable ground planes near the discharge that could divert it from the desired path. This problem could be aggravated because sodium has a low ionization potential and the background ionization level could be high unless the temperature can be kept fairly low. Another question that requires further examination is the effect of the argon buffer gas on the discharge guiding process. Finally, because of the practical problems associated with handling the sodium, it would be worthwhile to search for a more benign gas to use in this process. A search of molecular gases may be fruitful in this regard.

III. FIRST WALL RESPONSE

First wall survivability is a critical problem to all ICF reactor designs. The largest potential for damage to the first wall of a light ion beam fusion reactor is not directly from the target explosion generated ions and X-rays because they will be stopped in the 10-100 Torr of cavity gas provided $Z > 10$.[30] However, the deposition of this energy into the gas creates a fireball which may propagate to the wall with its possibly damaging overpressure and flux of radiant heat. Since the characteristics of the fireball are to a large degree determined by the propagation of radiation through the gas, the heat fluxes and overpressure at the first wall of the reactor may be controlled by the optical properties of the cavity gas. In this section we show that a cavity gas of argon that would have a pressure of 50 Torr at 0°C mixed with 0-2% by volume of sodium vapor can provide adequate protection for a reactor first wall. The argon can easily stop the target generated X-rays and ion debris while the sodium controls the opacity of the gas.

To calculate the propagation of the fireball to the first wall of the reactor, it is necessary to first determine the opacity and the equation of state of the cavity gas. This is done with a computer code MIXER which is a variant of the previously reported MFP code.[31] The atomic physics of a monatomic gas is modeled by assuming that the average ionization state follows the Saha formalism and that the six most populous ionization states have densities spread in a Gaussian about the average. The first twenty atomic energy levels are included where their populations are assumed to obey Boltzmann's law. In the Saha model, recombination is through three body recombination so that the ionization state of a minority species, sodium in this case, whose density is much smaller than that of the majority species is very different from what it would be if the majority species was not present. For this reason, we cannot calculate the properties of the gas separately for each species and then combine them in some manner but must calculate the properties of the combined gases for each different concentration of sodium. Once the equation of state of the gas has been calculated, the Rosseland and Planck averaged mean free paths for radiation are calculated considering photo-ionization, inverse Bremsstrahlung, atomic line absorption and Thompson scattering as photon stopping mechanisms.[32]

This analysis shows that, as long as one considers photons with energies greater than the first ionization potential, photo-ionization is the dominant mechanism of photon stopping. When the photon energy drops below this energy, the absorption coefficient drops by several orders of magnitude so that the gas is relatively transparent to low energy photons. An inert gas like argon with a high value for the first ionization energy will be transparent to much higher energy photons than an alkali metal vapor like sodium. Thus, the

addition of a small amount of sodium will not significantly change the opacity of the gas to higher energy photons but will greatly increase the opacity to low energy photons. This is demonstated in Fig. 3, a plot of the Planck mean free path versus the plasma temperature for the case when the radiation is in equilibrium with the plasma. This shows that, when the photons are of low energy, increasing amounts of sodium rapidly increase the photon stopping ability of gas.

Once the optical properties of the gas are known, the physics of the fireball propagation may be studied.[33] As stated earlier, the argon will absorb target generated X-rays and ion debris in a small volume, creating a hot fireball at the center of the cavity which is surrounded by cold gas. Initially, the radiation mean free paths are long in the fireball but short in the cold gas so that a wave of heat moves into the cold gas by successive warming of layers of gas near the fireball. Initially, this heating wave, whose speed decreases with decreasing fireball temperature, propagates more rapidly than the sound speed. As the fireball expands and cools, the speed of the heating wave drops to the speed of sound and a shock wave is formed which breaks away from the fireball. The fireball continues expanding and cooling until the mean free paths for fireball radiation in the cold gas are longer than the distance to the first wall, at which time the fireball begins radiating its energy to the wall. This continues until the fireball cools to the point where it no longer contains significant radiant energy and the flow of radiant energy ceases. The effect of decreasing the mean free paths to low energy photons in the cold gas is to slow the propagation of the radiation to the wall. Thus, by adjusting the opacity through variations in the sodium concentration, one may control the total amount of heat radiated to the wall per explosion and the rate at which this heat reaches the wall.

A hydrodynamic radiative transfer computer code, FIRE, has been used to simulate this behavior in fireballs.[34] FIRE is a one-dimensional hydrodynamics code that calculates the dynamics of two fluids; the plasma at its own temperature and the radiation at its own temperature. The transport of the radiation fluid is flux limited and upstream averaged. The equation of state of the plasma and mean free paths of radiation in the gas are read from tables of data provided by the atomic physics code MIXER.

A series of fireball calculations have been performed with FIRE for a reactor cavity consistent with the laser breakdown requirements discussed in Section II. The parameters used and the results are outlined in Table I. The calculations have been done with sodium concentrations ranging from 0% to 2%. The most important results for first wall survivability are the radiant heat flux and the overpressure. These are shown for the largest (2%) and the smallest (0%) sodium concentations in Figs. 4 and 5 respectively. These results indicate that the heat flux for 2% sodium is held very effectively behind the shock front and that the first wall has an insignificant temperature rise. On the other hand, when the cavity gas is pure argon, the heat flux reaches the first wall long before the shock wave does and the heat flux reaches a much higher maximum. From these two calculations the effect of the sodium is evident and this becomes even more clear in Fig. 6, which is a plot of the total energy radiated (E_{out}), the maximum overpressure (ΔP), and the maximum heat flux (q_{max}) versus the sodium concentration. When the sodium concentration is near 0.2% the wall response is most sensitive to sodium concentration so we tried this as an operating point. The heat flux and overpressure for 0.2% sodium are shown in Fig. 7. This case has important advantages over the two previous cases because the maximum heat flux is low

TABLE I

Parameters and Results of Fireball Calculations

Wall Radius = 4 meters

Initial Gas Temperature = 0.1 eV

Argon Density = 1.8×10^{18} cm^{-3}

Initial Energy of Fireball = 30 MJ

	Sodium Concentration (%)				
	0.0	0.1	0.2	1.0	2.0
Energy Radiated* (MJ)	3.1	2.7	1.6	0.2	0.1
Shock Pressure (MPa)	0.195	0.233	0.255	0.327	0.332
Max. Heat Flux to Wall (kW/cm^2)	3.4	0.72	0.47	0.10	0.035

*Energy radiated to first wall in the first 2.5 msec following the target explosion

enough that the maximum wall temperature difference is tolerable (21.6 K for a 0.5 cm thick stainless steel wall) while the heat reaches the wall in a very broad pulse so that a significant energy can be extracted from the gas. For all three cases the overpressure is not large enough to cause structural problems in the reactor wall.[35]

IV. DISCUSSION AND CONCLUSIONS

From the discussions of Sections II and III, we are able to choose a set of cavity and first wall parameters consistent with laser induced channel formation and first wall protection. These parameters are shown in Table II. The reactor cavity is a right circular cylinder 4 meters in radius, and 8 meters in height where the channels are assumed to start 1 meter behind the first wall. The cavity is filled with 1.8×10^{18} cm^{-3} argon gas which contains an additional 0.2% of sodium vapor.

Forty channels for propagating 4 MeV light ions from diodes to the target are assumed to each have a beam area of 0.2 cm^2. From Fig. 2 we find that, with this sodium density, a 1.2 J laser tuned to the 589.6 nm sodium line and with a 100 nsec pulse width can form a channel through resonant absorption and super-elastic electron-ion collisions. This pulse width is much less than the 1 μsec time scale for turbulence. Thus, less than 50 J of laser energy are required for the reactor. A good candidate for such a laser is Rhodamine-6G dye driven by flash lamps. Thus, it is entirely feasible that channels may be formed via laser breakdown with a realistic amount of energy.

These channels allow the ion beams to implode the fusion target which is assumed to release 30% of its 100 MJ yield in the form of X-rays and ions. The 1.8×10^{18} cm^{-3} argon will stop this energy within 10 cm of the target, creating a uniform 10 cm radius 30 MJ fireball. This propagates to the first

TABLE II

Parameters Consistent with Channel Formation and First Wall Protection

First Wall Radius	4 meters
Channel Length	5 meters
Rep Rate	10 Hz
Argon Density	1.8×10^{18} cm^{-3}
Sodium Concentration	0.2%
Channel Area	0.2 cm^2
Number of Beams	40
Laser Energy/Beam	1.2 J
Laser Pulse Width	100 nsec
Laser Wavelength	589.6 nm
Laser Type	Flash Lamp Driven Rhodamine-6G
Target Generated X-ray and Ion Energy	30 MJ
Initial Fireball Radius	10 cm
Radiant Heat to First Wall (in 2.5 msec)	1.6 MJ
Maximum Heat Flux to Wall	470 W/cm^2
Pulse Width of Radiant Heat Flux	1.5 msec
Shock Overpressure at Wall	0.257 MPa
Cell Wall Thickness	0.5 cm
Total Wall Thickness	5.0 cm
Wall Material	HT-9
Maximum Wall Temperature Rise	15.1 K
Maximum Thermal Stress	36.89 MPa
Maximum Mechanical Stress	138 MPa

wall, depositing radiant energy and imposing pressure as shown in Fig. 7. The total radiant heat deposited in the first 2.5 msec is 1.6 MJ, where much of it arrives in a pulse 1.5 msec wide centered around a peak flux of 470 W/cm^2. The first wall is assumed to be made of the ferritic steel HT-9. It has coolant channels with 0.5 cm thick walls and a coolant temperature of 573 K. A transient temperature diffusion calculation code predicts that the maximum difference in temperature across the channel wall is 15.1 K. Using this temperature distribution,a transient thermal stress calculation predicts that the maximum thermal stress in the wall is a 36.89 MPa compressional stress on the front surface. The tensile yield strength of HT-9 is 400 MPa, well above the calculated thermal stress. Englestad and Lovell[35] have shown that this first wall of HT-9 can be designed to sustain the 0.257 MPa overpressure. Thus this cavity gas adequately protects the first wall from target generated ions and X-rays.

There are several questions pertaining to channel formation and first wall protection that remain unanswered. It is unknown what efficiency is possible for the creation of channels. The quoted value of 1.2 J per beam line is the usable laser energy. If the bandwidth of the laser is larger than that of the sodium line, the process will become less efficient. The absorption line will be affected by collisional and Doppler broadening. Before the efficiency can be determined these details as well as the laser bandwidth and efficiency must be faced.

Another question which must be faced is the question of convective heat transfer to the first wall. Since the majority of the fireball energy is not radiated to the wall but is held in the gas, convective heat transfer may play a large role in the energy budget of the reactor. We expect that this heat

transfer will not be of a sharply pulsed nature and should not have a great influence on the peak thermal stresses in the first wall. It will determine the final temperature of the cavity gas and this will affect the channel formation process.

These and other unanswered questions indicate that this study should be of a continuing nature. However, we feel that the answers to these additional considerations will not fundamentally affect our general conclusion that our choice of cavity gas simultaneously allows laser initiated channel formation and first wall protection.

ACKNOWLEDGMENT

This work was supported by Sandia Laboratory under Contracts 13-9841 and 13-9838.

References

1. J. Nuckolls, L. Wood, A. Thiessen, and G. Zimmerman, "Laser Compression of Matter to Super High Densities: Thermonuclear (CTR) Applications," Nature, 239, (1972).

2. Physics Today, 32, 11, p. 20-22 (Nov. 1979).

3. G. Yonas, J. Poukey, K. Prestwich, J. Freeman, A. Toepfer, and M. Clauser, Nucl. Fusion, 14, 731 (1974).

4. G. Yonas, "Fusion Power with Particle Beams," Sci. Amer., 239, 50 (Nov. 1978).

5. R. Bangerter and D. Meeker, "Ion Beam Inertial Fusion Target Designs," Lawrence Livermore Laboratory Report UCRL-78474 (1976).

6. D. Cook and M. A. Sweeney, "Design of Compact Particle-Beam-Driven Inertial Confinement Fusion Reactors," Proc. of the ANS Third Topical Mtg. on the Technology of Controlled Nuclear Fusion, Santa Fe, NM, 1178 (1978).

7. J. N. Olsen, D. J. Johnson, and R. J. Leeper, "Propagation of Light Ions in a Plasma Channel," Appl. Phys. Lett., 36, 808-810 (1980).

8. S. I. Abdel-Khalik, G. A. Moses, and R. W. Conn, "Engineering Problems of Laser Driven Fusion Reactors," Nucl. Tech., 43, 5 (1979).

9. F. L. Sandel, F. C. Young, S. J. Stephanakis, F. W. Oliphant, G. Cooperstein, Shyke A. Goldstein, and D. Mosher, "Ion Beam Transport in Plasma Channels," Bull. Amer. Phys. Soc., 24, 1031 (1979).

10. J. R. Freeman, L. Baker, P. A. Miller, L. P. Mix, J. N. Olsen, J. W. Poukey, and T. P. Wright, "Electron and Ion Beam Transport to Fusion Targets," SAND-79-0734C, Sandia Laboratories (1979).

11. Donald L. Cook, Sandia Laboratories, private communication, December 1979.

12. C. Grey Morgan, "Laser-Induced Breakdown of Gases," Rep. Prog. Phys., 38, 621-665 (1975); and E. Panarella, "Theory of Laser-Induced Gas Ionization," Foundations Phys., 4, 227-259 (1974).

13. F. S. Felber, "Fast-Moving Laser Focus," Appl. Phys. Lett., 36, 723-725 (1980).

14. H. L. Rutkowski, D. W. Scudder, Z. A. Pietrzyk, and G. C. Vlases, "CO_2 Laser Heating of Plasma Columns in a Steady Solenoid Field," Appl. Phys. Lett., 26, 421-423 (1975).

15. A. A. Offenberger, M. R. Cervenan, and P. R. Smy, "CO_2-Laser-Produced Plasma Columns in a Solenoidal Magnetic Field," J. Appl. Phys., 47, 494-497 (1976).

16. L. C. Johnson and T. K. Chu, "Measurements of Electron Density Evolution and Beam Self-Focusing in a Laser-Produced Plasma," Phys. Rev. Lett., 32, 517-520 (1974); and T. K. Chu and L. C. Johnson, "Measurements of the Development and Evolution of Shock Waves in a Laser-Induced Gas Breakdown Plasma," Phys. Fluids, 18, 1460-1466 (1975).

17. R. E. Pechacek, "Laser Guided, High Current, Linear Discharge," Bull. Amer. Phys. Soc., 17, 593 (1972).

18. J. R. Greig, D. W. Koopman, R. F. Fernsler, R. E. Pechacek, I. M. Vitkovitsky, and A. W. Ali, "Electrical Discharges Guided by Pulsed CO_2-Laser Radiation," Phys. Rev. Lett., 41, 174-177 (1978).

19. M. Raleigh, J. D. Sethian, L. Allen, J. R. Greig, R. B. Fiorito, and R. F. Fernsler, "Experiments on the Injection of Relativistic Electron Beams into Preformed Channels in the Atmosphere," NRL Memorandum Report 4220 (1980).

20. M. Raleigh, J. C. Halle, R. E. Pechacek, R. B. Fiorito, E. Laikin, and J. R. Greig, "Reduced Density Current Carrying Channels for Transporting Charged Particle Beams," IEEE International Conference on Plasma Science, Madison, WI (1980).

21. K. A. Saum and D. W. Koopman, "Discharges Guided by Laser-Induced Rarefaction Channels," Phys. Fluids, 15, 2077-2079 (1972).

22. R. V. Ambartsumyan, V. S. Letokhov, G. N. Makarov, and A. A. Puretskii, "Investigation of Vibrationally Excited Ammonia Molecules by the Double IR-UV Resonance Technique," Sov. Phys. - JETP, 41, 871-876 (1976); Hyung Kyu Shin, "Vibration-to-Rotation Energy Transfer in Water, Heavy Water, and Ammonia," J. of Phys. Chem., 77, 346-351 (1973); and H. E. Bass and T. G. Winter, "Vibrational and Rotational Relaxation in Ammonia," J. of Chem. Phys., 56, 3619-3623 (1972).

23. T. B. Lucatorto, "Efficient Laser Production of a Na^+ Ground-State Plasma Column: Absorption Spectroscopy and Photo-ionization Measurement of Na^+," Phys. Rev. Lett., 37, 428-431 (1976).

24. T. J. McIlrath and T. B. Lucatorto, "Laser Excitation and Ionization in Dense Li Vapor: Observation of the Even-Parity, Core-Excited Auto-ionizing States," Phys. Rev. Lett., 38, 1390-1393 (1977).

25. A. C. Tam and W. Happer, "Plasma Production in a Cs Vapor by a Weak Laser Beam at 6010 Å," Opt. Commun., 21, 403-407 (1977).

26. R. M. Measures, N. Drewell, and P. Cardinal, "Electron- and Ion-Beam Transportation Channel Formation by Laser Ionization Based on Resonance Saturation-LIBORS," J. Appl. Phys., 50, 2662-2669 (1979).

27. R. M. Measures, N. Drewel, and P. Cardinal, "Laser Interaction Based on resonance Saturation (LIBORS): An Alternative to Inverse Bremsstrahlung for Coupling Laser Energy into a Plasma," Appl. Opt., 18, 1824-1827 (1979).

28. M. Maeda, O. Uchino, T. Okada, and Y. Miyazoe, "Powerful Narrow-Band Dye Laser Forced Oscillator," Jap. J. Appl. Phys., 14, 1975-1980 (1975); F. N. Baltakov, B. A. Barikhin, and L. V. Sukhanov, "400-J Pulsed Laser Using a Solution of Rhodamine-6G in Ethanol," JETP Lett., 19, 174-175 (1974); and T. Okada, M. Maeda, and Y. Miyazoe, "Spectral Narrowing of a Flashlamp-Pumped High-Energy Dye Laser by Two-Stage Injection Locking," IEEE J. of Quantum Electr., QE-15, 616-623 (1979).

29. 1980 Laser Focus Buyer's Guide, p. 154.

30. D. L. Cook and M. A. Sweeney, private communication, January, 1979.

31. R. R. Peterson and G. A. Moses, "MFP - A Calculation of Radiation Mean Free Paths, Ionization and Internal Energies in Noble Gases," University of Wisconsin Fusion Engineering Program Report UWFDM-307 (1979) (accepted for publication in Computer Physics Communications).

32. V. Zeldovich and Yu. Raizer, Physics of Shock Waves and High Temperature Hydrodynamic Phenomena, Academic Press (New York, 1966), Chapter V.

33. Detailed discussions of the physics of fireballs may be found in G. A. Moses and R. R. Peterson, "First Wall Protection in Particle Beam Fusion Reactors by Inert Cavity Gases," (accepted for publication in Nuclear Fusion) and references therein.

34. R. R. Peterson and G. A. Moses, "Blast Wave Calculations in Argon Cavity Gas for Light Ion Beam Fusion Reactors," University of Wisconsin Fusion Engineering Program Report UWFDM-315 (October 1979).

35. R. L. Engelstad and E. G. Lovell, "First Wall Mechanical Design for Light Ion Beam Fusion Reactors," University of Wisconsin Fusion Engineering Program Report UWFDM-322 (December 1979).

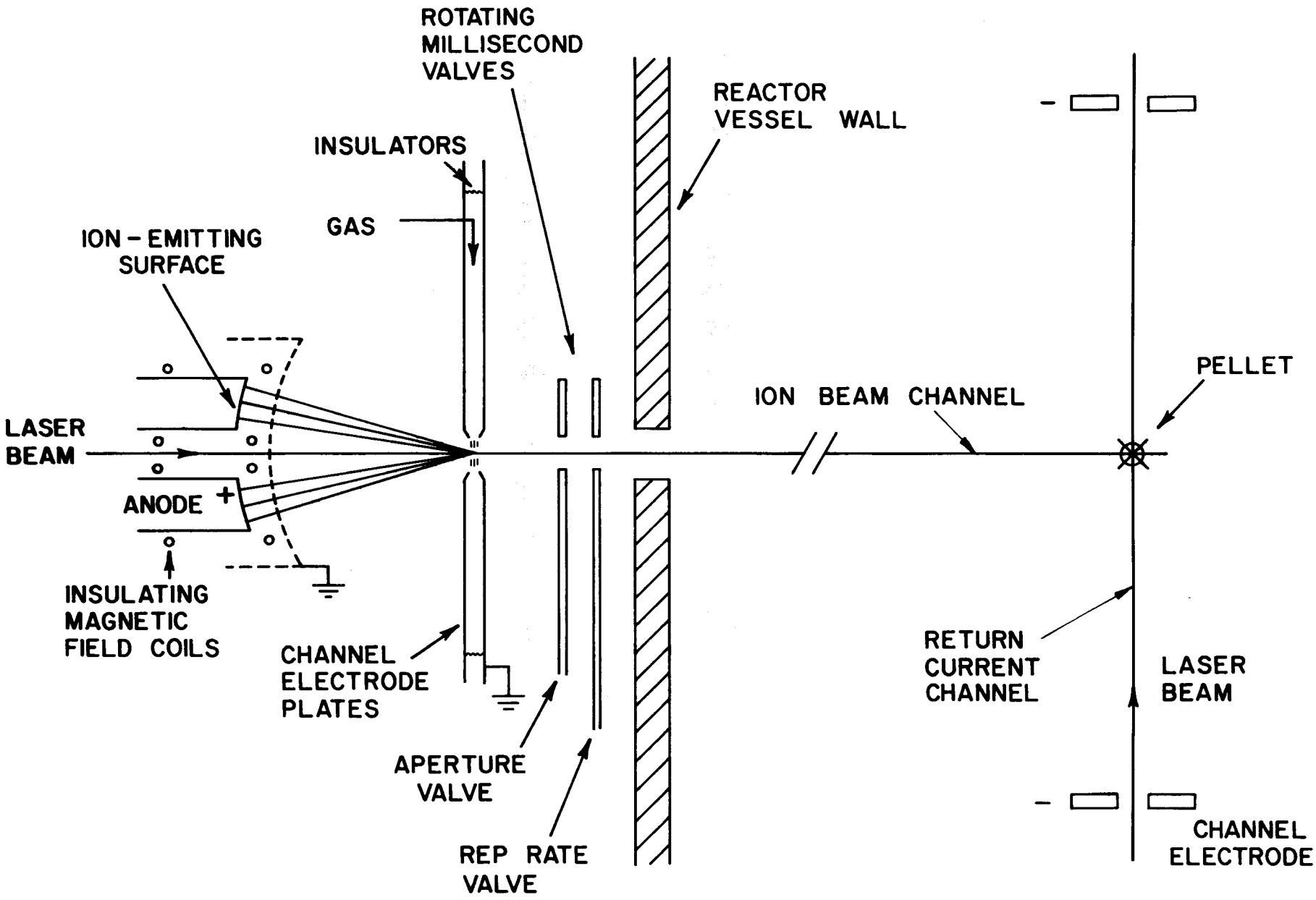

Figure 1. Schematic Diagram of Light Ion Beam and Laser Breakdown System.

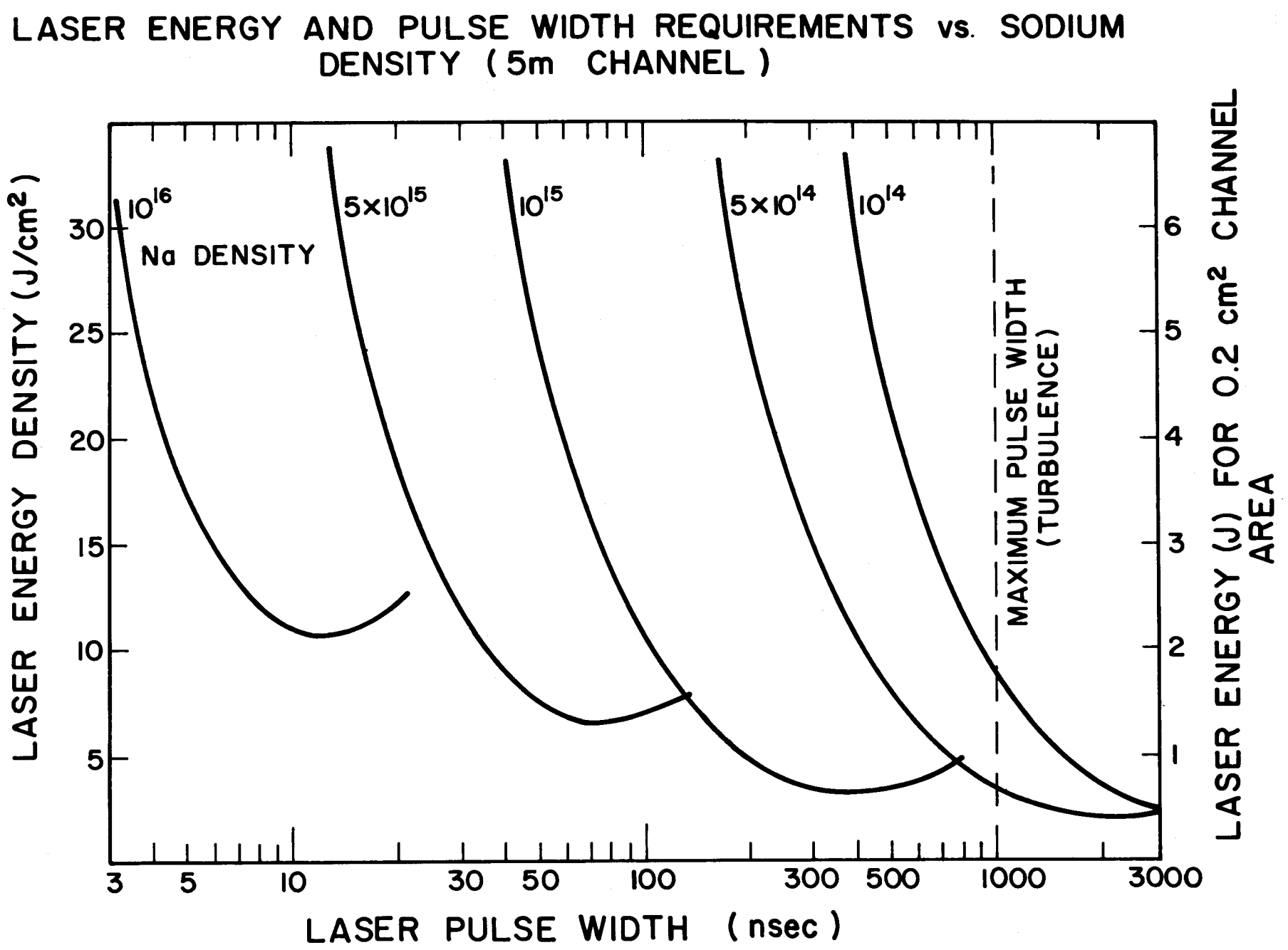

Figure 2. Laser Energy Density Requirements versus Laser Pulse Width for Various Sodium Densities.

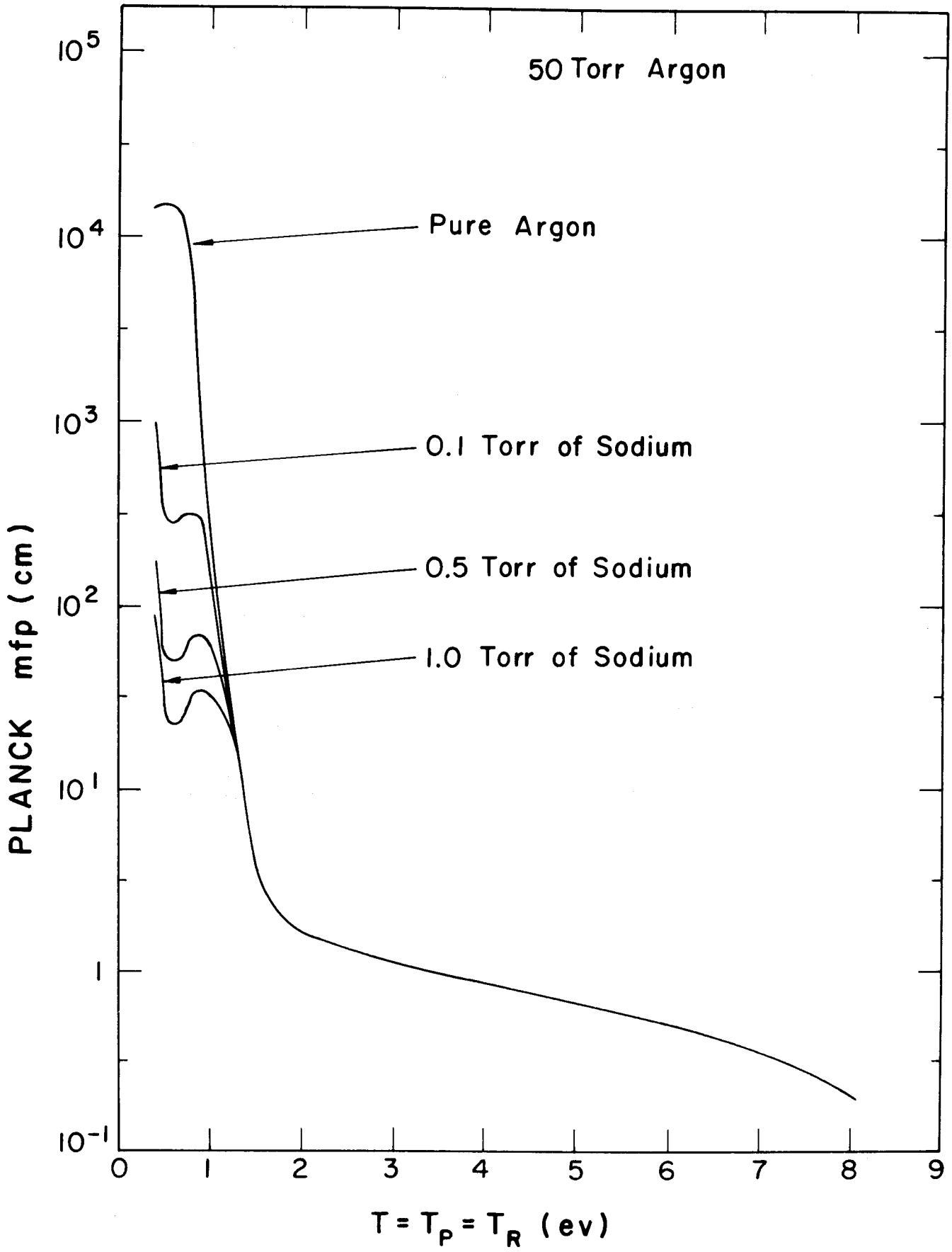

Figure 3. Planck Mean Free Path versus Temperature for Various Concentrations of Sodium Mixed with 1.8×10^{18} cm^{-3} Argon. Here the radiation is in equilibrium with the gas at temperature T.

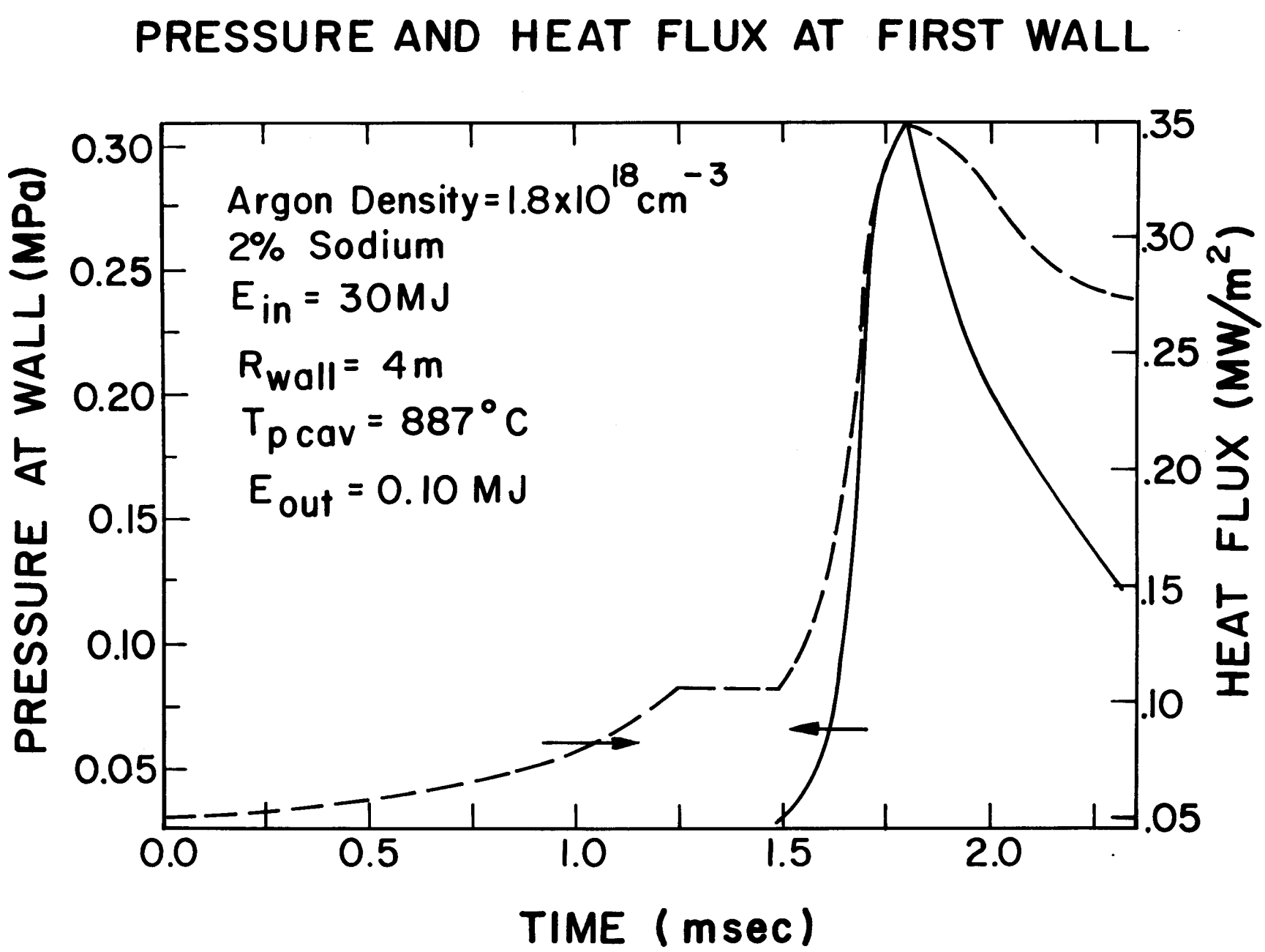

Figure 4. Pressure and Heat Flux at a 4 meter Radius First Wall versus Time. A 30 MJ explosion sends a blast wave through 1.8 x 10^{18} cm^{-3} of 0.1 eV argon gas which is mixed with 2% by volume of sodium.

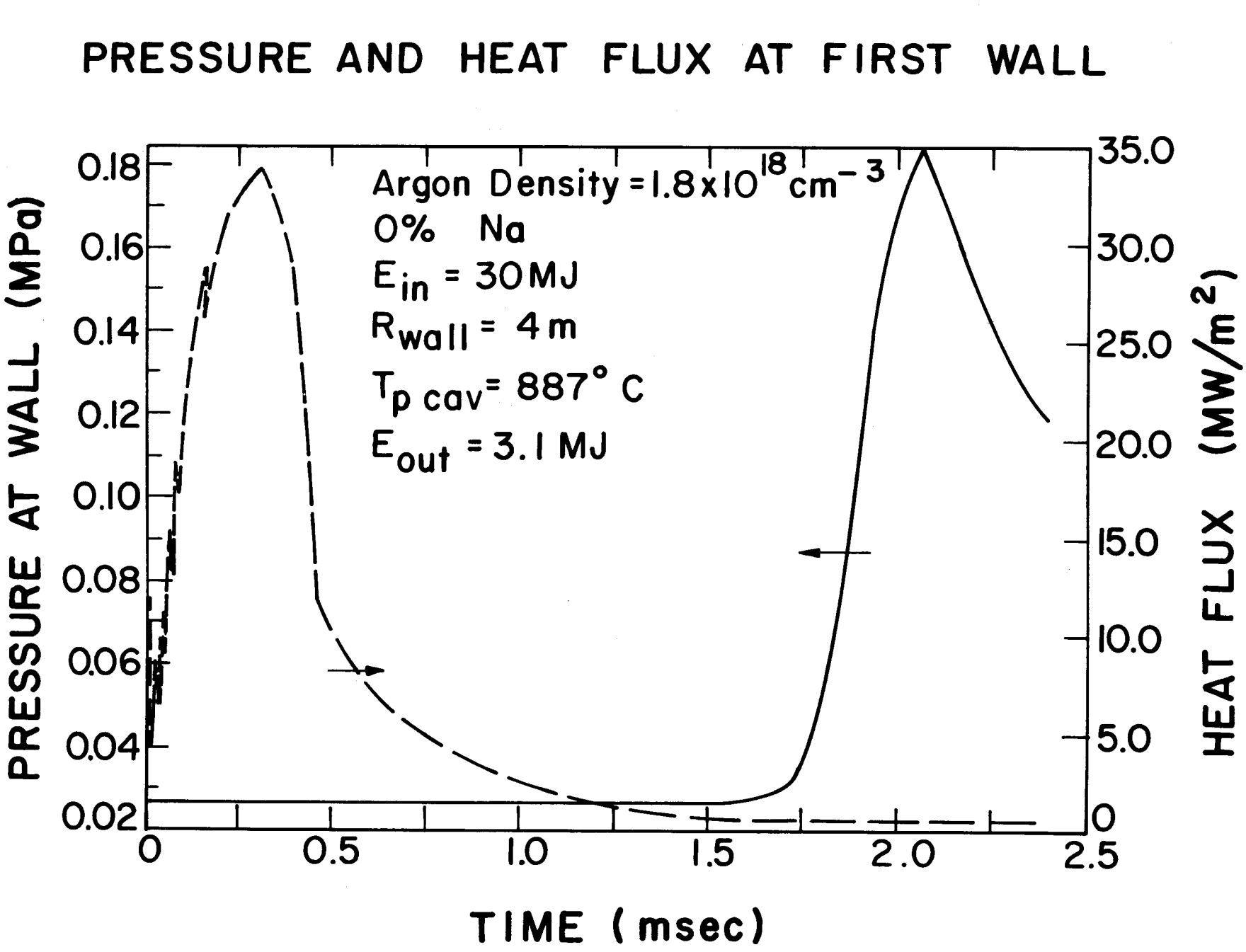

Figure 5. Pressure and Heat Flux at a 4 meter Radius First Wall versus Time. This case is the same as Fig. 4 except that the gas is pure argon.

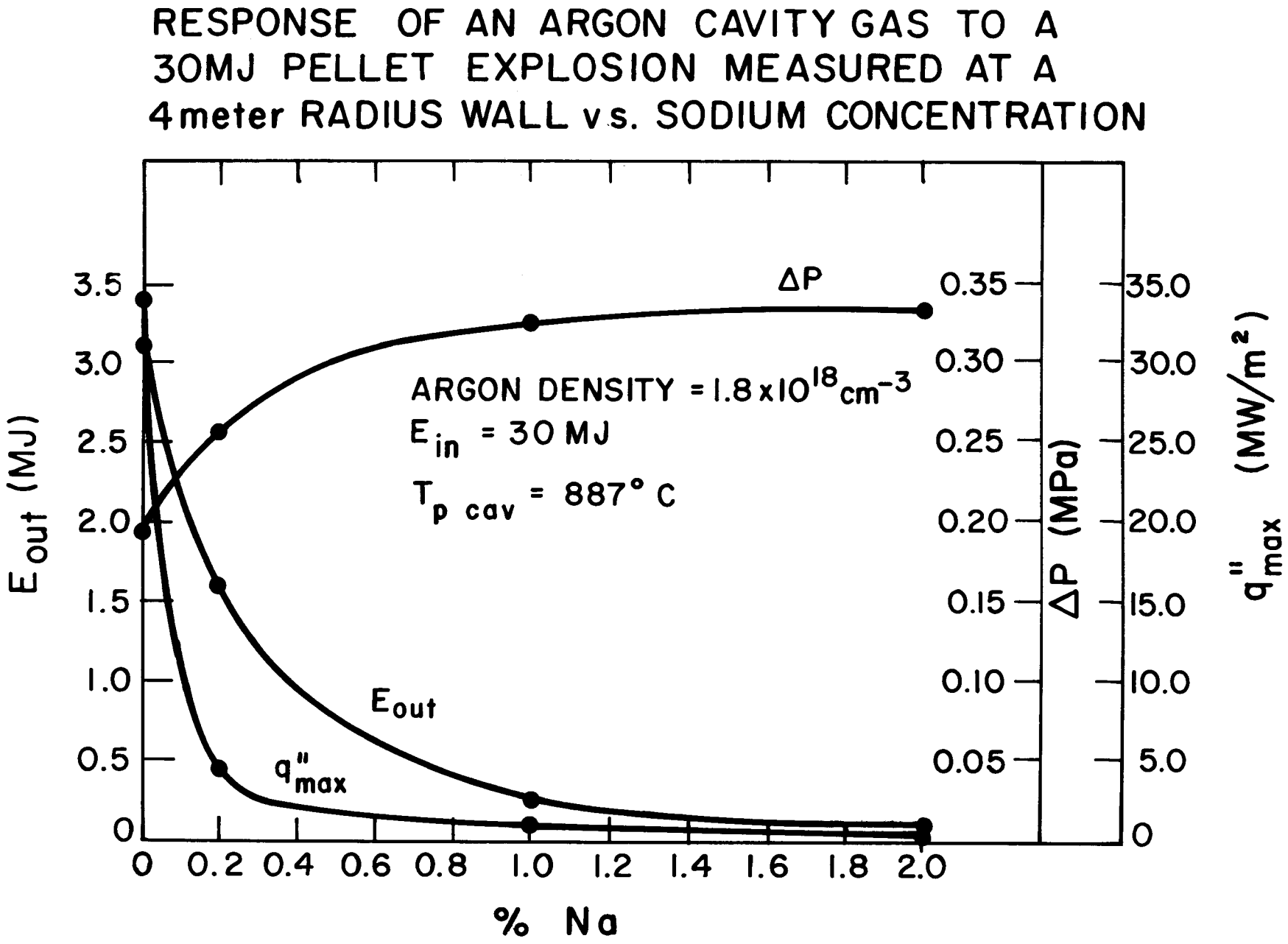

Figure 6. Maximum Overpressure, Maximum Heat Flux and Energy Radiated in the First 2.5 msec at a 4 meter Radius First Wall versus Sodium Concentration. Everything but the sodium concentration is the same as in Fig. 4.

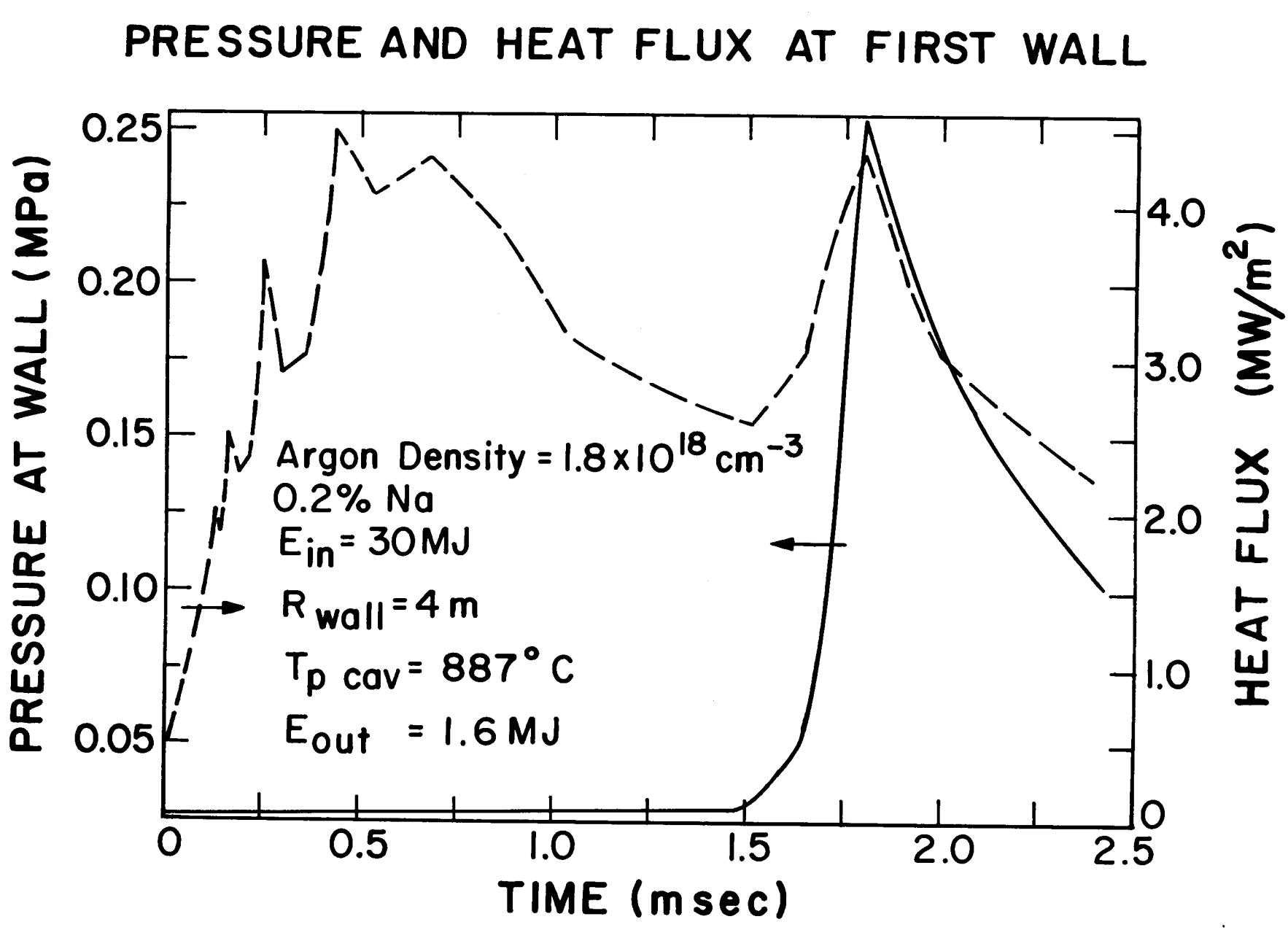

Figure 7. Pressure and Heat Flux at a 4 meter Radius First Wall. This case is the same as Fig. 4 except that the sodium concentration is 0.2%.